

1 **Changes in the Subchondral Bone Affect Pain in the Natural Course of Traumatic**  
2 **Articular Cartilage Defects**

3 <sup>1</sup>Yuichi Kato, MD, <sup>1,2</sup>Tomoyuki Nakasa, MD, PhD, <sup>1</sup>Junichi Sumii, MD, <sup>1</sup>Munekazu Kanemitsu,  
4 MD, PhD, <sup>3</sup>Masakazu Ishikawa, MD, PhD, <sup>1,2</sup>Shigeru Miyaki, PhD, <sup>1</sup>Nobuo Adachi, MD, PhD

5

6 1. Department of Orthopaedic Surgery, Graduate School of Biomedical and Health Sciences,

7 Hiroshima University

8 2. Medical Center for Translational and Clinical Research, Hiroshima University Hospital

9 3. Department of Artificial Joints and Biomaterials, Graduate School of Biomedical and Health

10 Sciences, Hiroshima University

11

12 **Abstract**

13 **Objective:** Articular cartilage defect causes joint pain and finally progresses to  
14 osteoarthritis. Although the subchondral bone condition affects clinical outcomes of  
15 cartilage defects, the natural course of changes in subchondral bone and associated pain  
16 in full-thickness cartilage defects remain unknown. Therefore, we investigated the natural  
17 course of histological changes in subchondral bone and joint pain in cartilage defects  
18 using a rat model.

19 **Design:** Full-thickness cartilage defects were created at the medial femoral condyle of  
20 10-week-old male Sprague Dawley rats. Rats were sacrificed at 3, 7, 14, 28, and 56 days  
21 postoperatively, and histological including immunohistochemistry and TRAP staining  
22 and micro-computed tomography ( $\mu$ CT) analyses of their knees were performed. Pain  
23 was evaluated using behavioral analysis and immunofluorescence staining of the dorsal  
24 root ganglion (DRG).

25 **Results:** The contour of the subchondral bone plate was maintained until day 3, but it was  
26 absorbed just under the cartilage defect from day 7 to 14. Starting on day 28, sclerotic  
27 changes surrounding the bone absorption area were detected. In the subchondral bone,  
28 the number of TRAP-positive cells peaked on day 14. Osteocalcin-positive cells were  
29 observed at 7 days, and their number gradually increased till day 56. Behavioral analysis  
30 showed that the total distance and the number of getting up by hind legs decreased on day  
31 14. The number of calcitonin gene-related peptide-positive fibers in the DRG increased  
32 and was the highest on day 14.

33 **Conclusions:** The subchondral bone condition under cartilage defects dynamically  
34 changes from bone resorption to sclerosis and is related to pain level.

35

36 **Key terms:** articular cartilage defect; subchondral bone; pain

37

38 **Introduction**

39 Articular cartilage provides smooth joint movement and weight-bearing capabilities  
40 through its ability to absorb stress, and reduce friction, and its high resistance to wear.<sup>1</sup> In  
41 the clinical setting, articular cartilage injuries are often associated with joint injuries, such  
42 as ligament injury, joint dislocation, and fracture. It is difficult for articular cartilage to  
43 heal spontaneously as it is poorly vascularized and innervated, and the injury eventually  
44 progresses to osteoarthritis (OA), especially in lesions that are greater than 1.5 cm in  
45 diameter.<sup>2</sup> The homeostasis of articular cartilage is maintained by the subchondral bone,  
46 with interactions such as nutritional exchange and coordination of load distribution taking  
47 place.<sup>3</sup> Therefore, damage to the articular cartilage layer significantly affects the  
48 condition of the subchondral bone, and may introduce both sclerotic and porotic changes.  
49 Articular cartilage injury also induces joint pain, which causes functional disability of the  
50 joint and decreases daily activity.<sup>4</sup> Although pain originates from the synovium and  
51 subchondral bone, the experience of pain in the subchondral bone is crucial because it is  
52 directly affected by load-bearing. Thus, articular cartilage defects should be treated  
53 appropriately to improve activities of daily living by removing pain and inhibiting the  
54 progression of OA.

55           Appropriate treatment of articular cartilage injury is selected, according to the size  
56 of the lesion and the condition of the subchondral bone.<sup>5</sup> The bone marrow stimulation  
57 (BMS) technique is generally performed because of its simplicity. However, it has been  
58 reported to have poor long-term clinical outcomes due to fragile fibrocartilage tissue  
59 covering the cartilage defect.<sup>6</sup> Moreover, intralesional osteophytes and subchondral bone  
60 cysts have been reported as complications with this technique.<sup>7</sup> BMS induces  
61 endochondral ossification around the bone hole in the subchondral bone, altering bone  
62 metabolism and thus causing excessive osteogenesis and bone resorption in the  
63 subchondral bone, which affects clinical outcomes after surgery.<sup>8</sup> Autologous  
64 chondrocyte implantation may also be used to treat articular cartilage injury, although it  
65 was reported that the condition of the subchondral bone affects the clinical outcome.<sup>7</sup>  
66 Since the condition of the subchondral bone influences on the clinical outcomes, it is  
67 important to understand the changes in the subchondral bone after cartilage injury.  
68 However, the timeline of histological changes that take place in the subchondral bone after  
69 cartilage injury remains unclear. If the subchondral bone condition changes in the natural  
70 course of a cartilage injury and postoperative outcomes are affected by the condition of  
71 the subchondral bone, the timing of surgery and the selection of the surgical procedure  
72 are crucial. In addition to using imaging technology such as computed tomography (CT),

73 to evaluate the condition of the bone, using joint pain as an indicator of the subchondral  
74 bone condition would be a useful technique for treating articular cartilage injury. Dynamic  
75 changes in osteoclast and osteoblast differentiation occur in the subchondral bone during  
76 the pathogenesis of osteochondral lesion (OCL) and OA.<sup>9,10</sup> An increase in the activity of  
77 osteoclasts leads to a decrease in the threshold of the pain, and nociceptive nerve fibers,  
78 including neuropeptides, increase the subchondral bone in OA and OCL. Several studies  
79 also showed a significant relationship between joint pain and the subchondral bone  
80 condition in articular cartilage damage in the OA model. It is reported that inhibition of  
81 subchondral bone deterioration by bisphosphonate could alleviate joint pain in rat OA  
82 models.<sup>11</sup> Another report demonstrated that improving joint pain was reduced as the  
83 subchondral bone microarchitecture was improved by the treatment of the intermittent  
84 parathyroid hormone in the OA mice models.<sup>12</sup> Based on these two factors, we  
85 hypothesized that the subchondral bone condition would change dynamically after an  
86 injury to the articular cartilage and that the condition of the subchondral bone would affect  
87 pain at the joint. The purpose of this study was, therefore, to elucidate the histological  
88 changes in the subchondral bone after articular cartilage injury in the weight-bearing area  
89 and to investigate the relationship between the subchondral bone condition and pain using  
90 a rat model.

91

92 **Methods**

93 This study was performed in accordance with the Guide for Animal Experimentation  
94 and was approved by the Committee of Research Facilities for Laboratory Animal  
95 Science (A19-159).

96

97 *Animals*

98 Twenty-five male 10-week-old Sprague-Dawley rats were used in this study. The  
99 animals were housed three per cage in the animal experimentation facility under a normal  
100 12-hour light-dark cycle with free access to food and water. Rats were anesthetized with  
101 an intraperitoneal injection of ketamine hydrochloride (1.4 mL/kg of body weight) and  
102 xylazine (0.4 mL/kg of body weight). Then right knee joints were exposed by a  
103 parapatellar approach, and 5.0 mm × 3.0 mm of full-thickness articular cartilage defects  
104 were created in the weight-bearing area of the medial femoral condyle using a surgical  
105 knife without any damage to the subchondral bone plate according to the procedure  
106 described in a previous report.<sup>13</sup> The left knee joints were used without procedure as the  
107 control group. An additional five male 10-week-old rats were incised to the joint capsule  
108 using the same method and used as a sham group for behavioral analysis. After surgery,

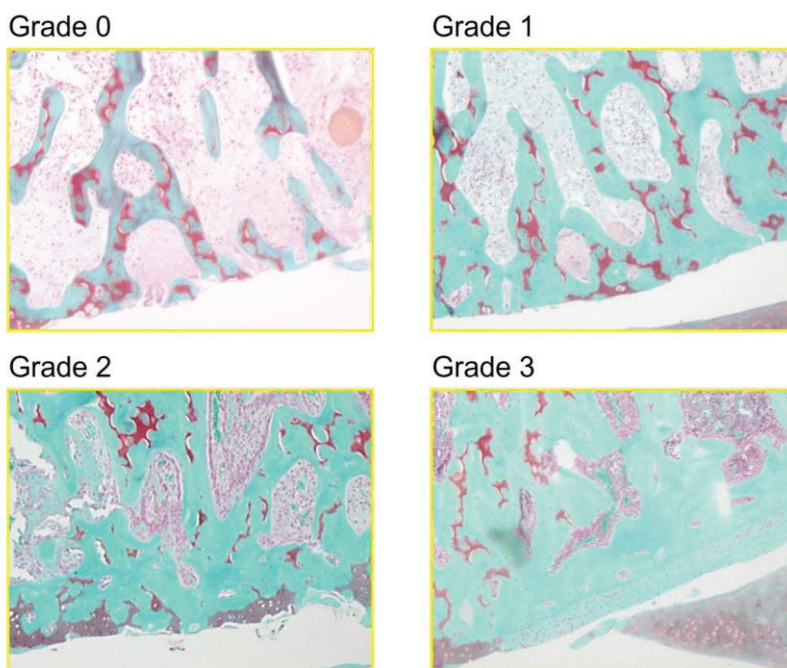
109 all rats were allowed to move freely inside the cages without load restriction. One week  
110 before sacrifice, 10  $\mu$ L of 2% Fluoro-gold (FG) (Fluorochrome Inc., Denver CO), a  
111 neuronal retrograde tracer, was injected into the knee joints.<sup>14</sup>

112

### 113 *Histological Assessment*

114 Five rats were sacrificed at each time point of 3, 7, 14, 28, and 56 days after surgery,  
115 and both knee joints and bilateral L4 dorsal root ganglions (DRGs) were harvested  
116 according to a procedure described previously report.<sup>15</sup> The knee joints were fixed in 4%  
117 paraformaldehyde phosphate-buffered saline (Wako Pure Chemical Industries Ltd.) for  
118 24 hours at 4 °C and then decalcified in distilled water containing 10%  
119 ethylenediaminetetraacetic acid for 3 weeks. Each sample was embedded in paraffin and  
120 cut into 4.5- $\mu$ m-thick sections along the sagittal plane, including the cartilage defect.  
121 Sections were stained using safranin-O/- fast green and hematoxylin-eosin (HE),  
122 according to standard protocols. Pathological changes in the subchondral bone below  
123 cartilage defects were graded by allocating a score ranging from 0 (best) to 3 (worst) to  
124 the subchondral bone using Aho's subchondral bone grading score.<sup>16</sup> A grade of 0,  
125 indicated that there was no evidence of subchondral bone sclerosis, and a grade of 3, that  
126 there was severe subchondral sclerosis and massively increased bone volume (Figure1).

127 Other sections were used for immunohistochemistry and tartrate-resistant acid  
128 phosphatase (TRAP) staining. The DRGs were fixed in 4% paraformaldehyde phosphate-  
129 buffered saline (Wako Pure Chemical Industries Ltd.) for 24 hours at 4 °C and then stored  
130 in 20% sucrose for 20 hours at 4°C. The DRGs were sliced into 8- $\mu$ m sections, using a  
131 Microm HM 520 cryostat.



132  
133 Figure 1. Aho's subchondral bone grading score. Representative images of Grades 0 – 3  
134 in the rat model. Grade 0; No evident subchondral bone sclerosis, thin subchondral bone  
135 plate and trabecular. Grade 1; Some subchondral sclerosis and bone volume is increased.  
136 Thickened bone trabeculae can be seen. Grade 2; A distinct increase subchondral sclerosis  
137 and bone volume. Grade 3; Severe subchondral sclerosis and massively increased bone  
138 volume. Subchondral bone plate flattens.

139

140 Each section from the knee was immunostained with an anti-osteocalcin (1:100  
141 dilution; Santa Cruz Biotechnology, Dallas, TX), anti-substance P (1:100 dilution; Santa  
142 Cruz Biotechnology, Dallas, TX), anti-calcitonin gene-related peptide (CGRP) (1:500  
143 dilution; Abcam, Cambridge, MA), using a 3,3'-diaminobenzidine substrate (Vector  
144 Laboratories). Osteocalcin-positive cells were evaluated at the trabecular edge, and the  
145 percentage of osteocalcin-positive cells was determined by the length of osteocalcin-  
146 positive cells divided by the length of the trabecular round, using Image J (National  
147 Institution of Health). TRAP staining was performed using a commercially available kit  
148 (Wako Pure Chemical Industries, Ltd., Osaka, Japan) according to the manufacturer's  
149 protocol. TRAP-positive multinucleated cells containing more than three nuclei were  
150 identified as osteoclasts.

151 CGRP expression and FG were assessed using fluorescence microscopy. Sections of  
152 DRGs were incubated with rabbit anti-CGRP (1:500; Abcam, Cambridge, MA) overnight  
153 at 4 °C, and the second detection was performed with Alexa Fluor 488-conjugated goat  
154 anti-rabbit secondary antibody (1:500 dilution) for 1 hour at room temperature. CGRP-  
155 positive nerve fibers and FG-positive fibers were counted, and the ratio of the number of  
156 CGRP and FG-positive cells to the number of FG-positive cells, determined using Image

157 J.

158

### 159 **Micro-Computed Tomography**

160 Samples were analyzed using high-resolution  $\mu$ -CT (SkyScan1176, Toyo Corporation,  
161 Tokyo, Japan) using the following parameters: tube voltage of 70 kV/360  $\mu$ A, Al 1-mm  
162 filter, and 18- $\mu$ m isotropic resolution. Images were reconstructed (NRecon, Toyo  
163 Corporation, Tokyo, Japan) for analysis using a CT analyzer (Toyo Corporation, Tokyo,  
164 Japan). The volume of interest was 5.0 mm  $\times$  3.0 mm and 1.0 mm deep in the subchondral  
165 bone lesion just below the cartilage defect, with the bone volume/tissue volume  
166 (BV/TV, %) ratio measured as previously described.<sup>17</sup>

167

### 168 **Open Field Test**

169 The open-field test was performed twice for each rat in a square arena (100 cm long,  
170 100 cm wide, 60 cm high), based on a previous experiment by Crumeyrolle-Arias et al.,<sup>18</sup>  
171 just before surgery and sacrifice. Briefly, each rat was placed in one corner of an open-  
172 field arena lit in the center (500 lx) and allowed to freely explore the arena. The  
173 movements of the rats were monitored and recorded for 6 minutes. The total distance the  
174 rat traveled in the arena and the number of times of rearing, getting up by hind legs, were

175 calculated using specific devices (SMART, Panlab SL, Barcelona, Spain).

176

## 177 **Statistical Analysis**

178 All results are expressed as mean and standard deviation. The Mann-Whitney U test  
179 was used to compare the total distance travelled and number of times rearing occurred  
180 that were measured during the open field test at each time point between the cartilage  
181 defect models and sham models. Tukey Kramer's post hoc test was used to compare  
182 subchondral bone grading, TRAP-positive and CGRP-positive ratio of subchondral bone,  
183 CGRP-positive ratio of DRG, and BV/TV ratio of subchondral bone among six groups.

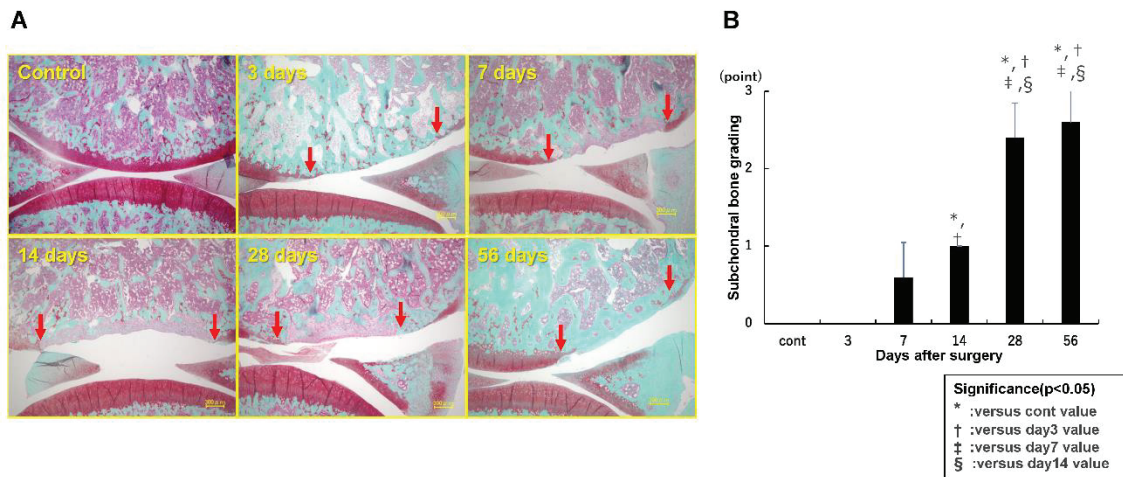
184

## 185 **Results**

### 186 *Subchondral Bone Changes after Cartilage Injury*

187 On day 3, the subchondral bone plate remained in all specimens and there was no  
188 obvious change in the subchondral bone with cartilage defect. On day 7, bone resorption  
189 was observed in the subchondral bone, which progressed until day 14. From days 28 to  
190 56, bone sclerosis gradually progressed in the subchondral bone (Figure 2A). Aho's  
191 grading score showed no significant difference until day 7, compared with the control  
192 group ( $0.0 \pm 0.0$ ,  $0.0 \pm 0.0$ , and  $0.6 \pm 0.4$  for the control group, and days 3 and 7,

193 respectively). From day 14, the score was gradually got worse ( $1.0 \pm 0.0$ ,  $2.4 \pm 0.4$ , and  
 194  $2.6 \pm 0.4$  for days 14, 28, and 56, respectively) (Figure 2B).



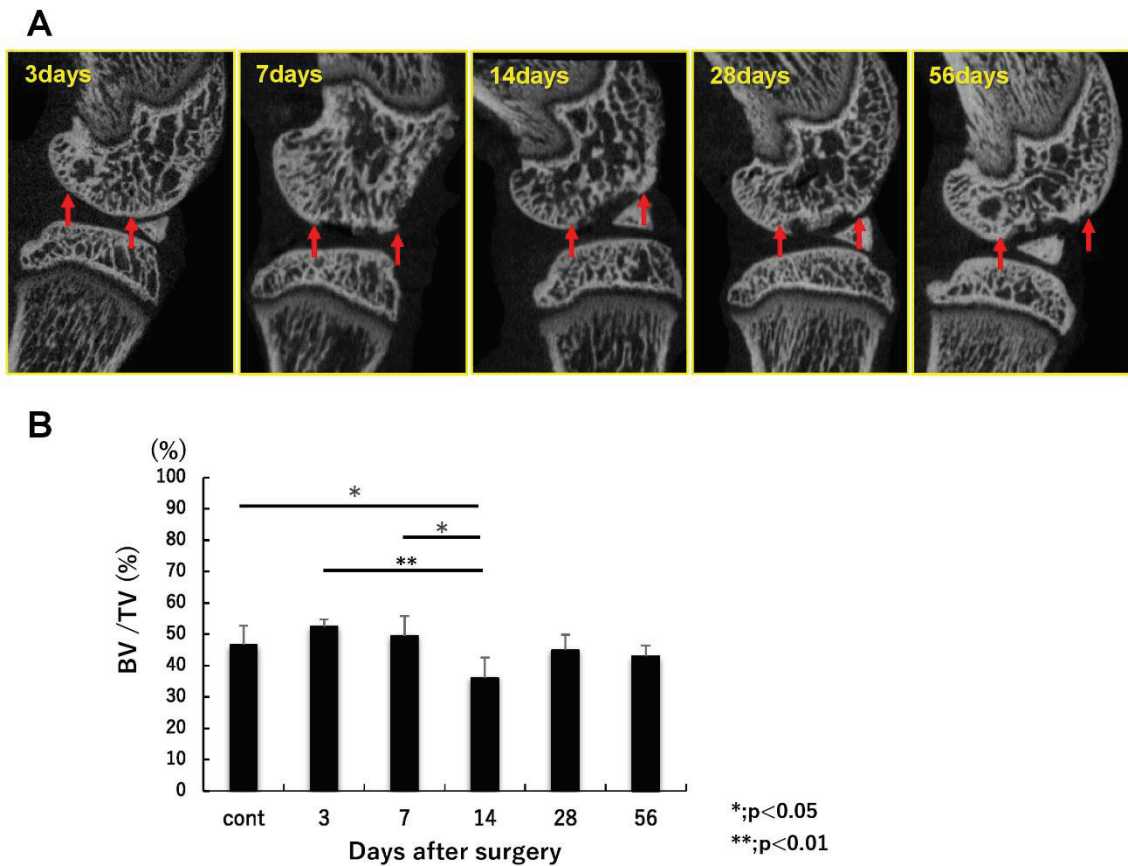
195

196 Figure 2. (A) histological evaluation: safranin-O staining, (B) subchondral bone grading.

197

198 The  $\mu$ -CT images showed that the contour of the subchondral bone plate was  
 199 maintained until day 3, but it was absorbed in the area just under the cartilage defect on  
 200 day 7. On day 14, the depth of the area of bone absorption expanded, and the subchondral  
 201 bone plate disappeared, but there was no sclerotic change at the site of the cartilage defect.  
 202 On day 28, osteogenesis in the subchondral bone defect filled towards the articular surface,  
 203 with sclerotic changes surrounding the bone absorption area. On day 56, the subchondral  
 204 bone defect was filled with sclerotic bone (Figure 3A). The BV/TV decreased  
 205 significantly on day 14 compared with the control group on day 3 and 7 ( $36.1 \pm 6.4\%$  vs.  
 206  $46.6 \pm 6.1\%$ ,  $52.5 \pm 2.2\%$ , and  $49.5 \pm 6.3\%$  for day 14, control group, days 3 and 7,

207 respectively), and then increased to levels similar to those of the control group after day  
208 28 ( $45.0 \pm 4.9\%$ , and  $42.9 \pm 3.5\%$  for days 28 and 56, respectively) (Figure 3B).

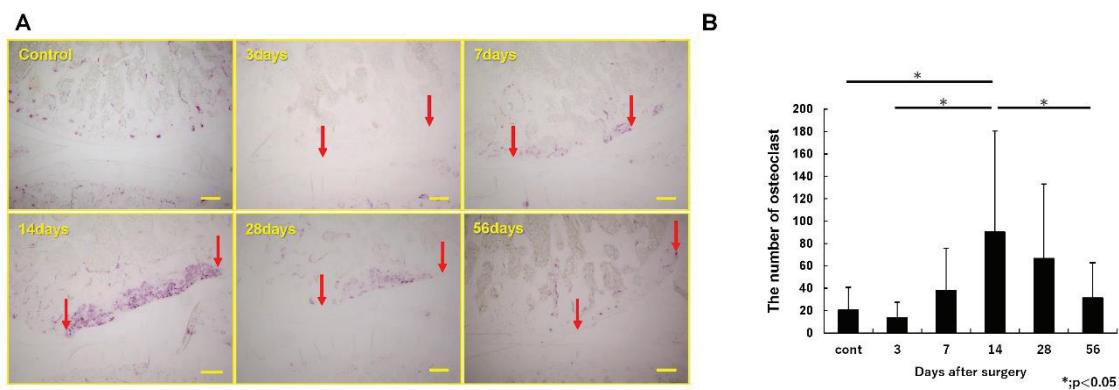


210 Figure 3. (A) micro-computed tomography( $\mu$ CT) findings of the knee, (B)the bone  
211 volume/tissue volume (BV/TV) ratio of the subchondral bone.

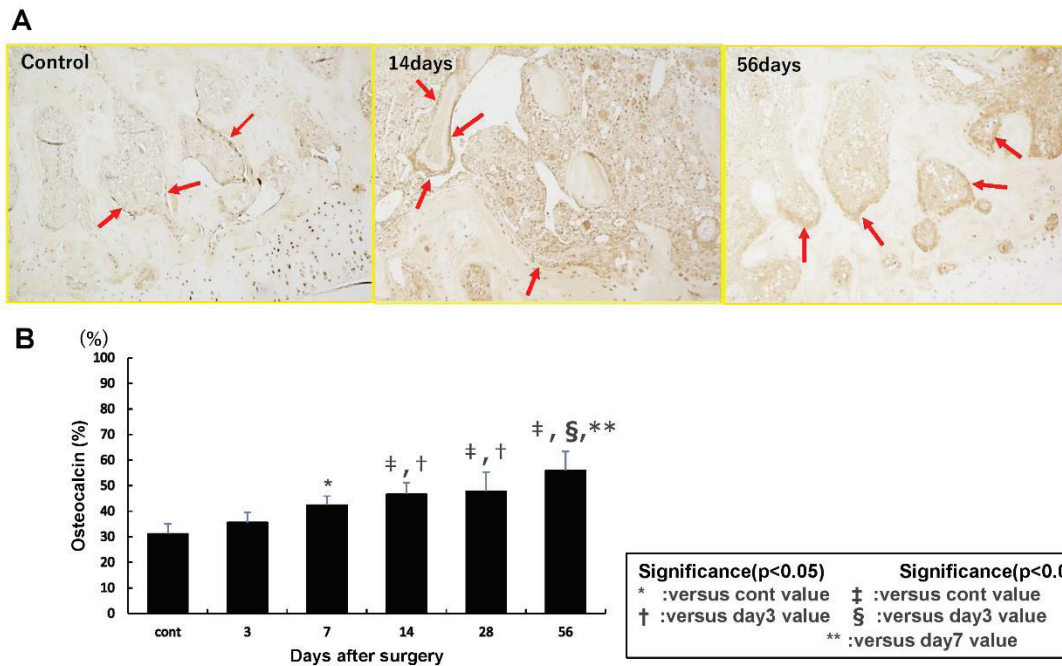
212

213 In the evaluation of the osteoclast activity in the subchondral bone, an increase in the  
214 number of osteoclasts in the subchondral bone just under the cartilage defect was  
215 observed from day 7, reaching a maximum on day 14, and then decreasing to levels  
216 similar to those observed in the control group by day 56. On day 14, the number was

217 significantly higher than that in the control group on days 3, 7, and 56 ( $90.2 \pm 23.9$  vs.  
 218  $20.4 \pm 5.0$ ,  $13.8 \pm 6.1$ , and  $37.8 \pm 14.8$  for days 14, control group, days 3, 7 and 56,  
 219 respectively) (Figure 4AB). With regard to osteogenesis, increasing numbers of  
 220 osteocalcin-positive cells in the subchondral bone were observed on day 7, and the  
 221 number gradually increased until day 56 ( $31.2\% \pm 3.8\%$ ,  $35.6\% \pm 4.0\%$ ,  $42.4\% \pm 3.4\%$ ,  
 222  $47.7\% \pm 7.6\%$ ,  $55.9\% \pm 7.4\%$  for the control group, days 3, 7, 14, 28, and 56, respectively).  
 223 On day 14, the osteocalcin-positive cells started accumulating, especially along the  
 224 trabecular around the cystic changes. From day 7, the percentage of osteocalcin-positive  
 225 cells was significantly more than that in the control group (Figure 5AB).



226  
 227 Figure 4. (A)osteoclast activity; TRAP staining (arrow: range of cartilage defect), (B)the  
 228 number of osteoclast at each time.



229

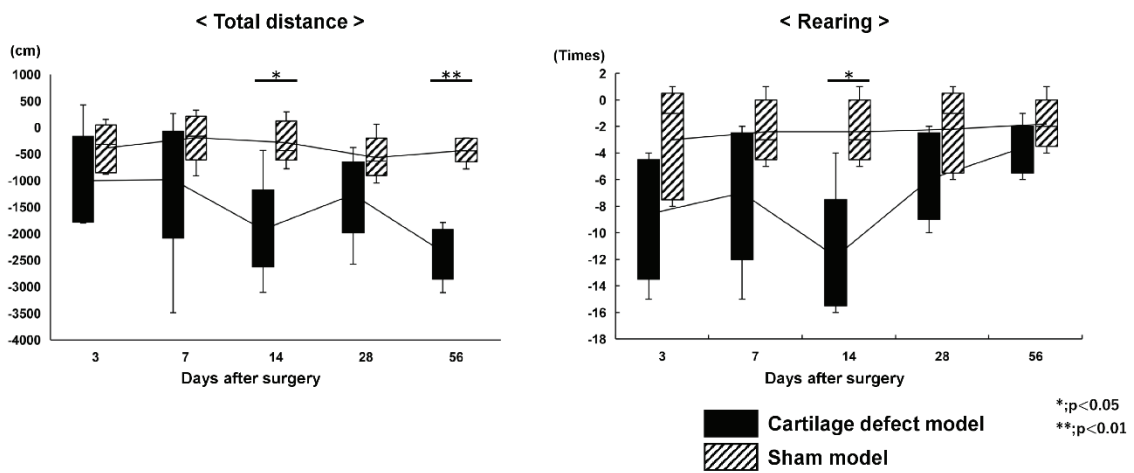
230 Figure 5. (A)osteoblast activity (arrow: osteocalcin-positive cells), (B)the percentage of  
 231 osteocalcin-positive cells.

232

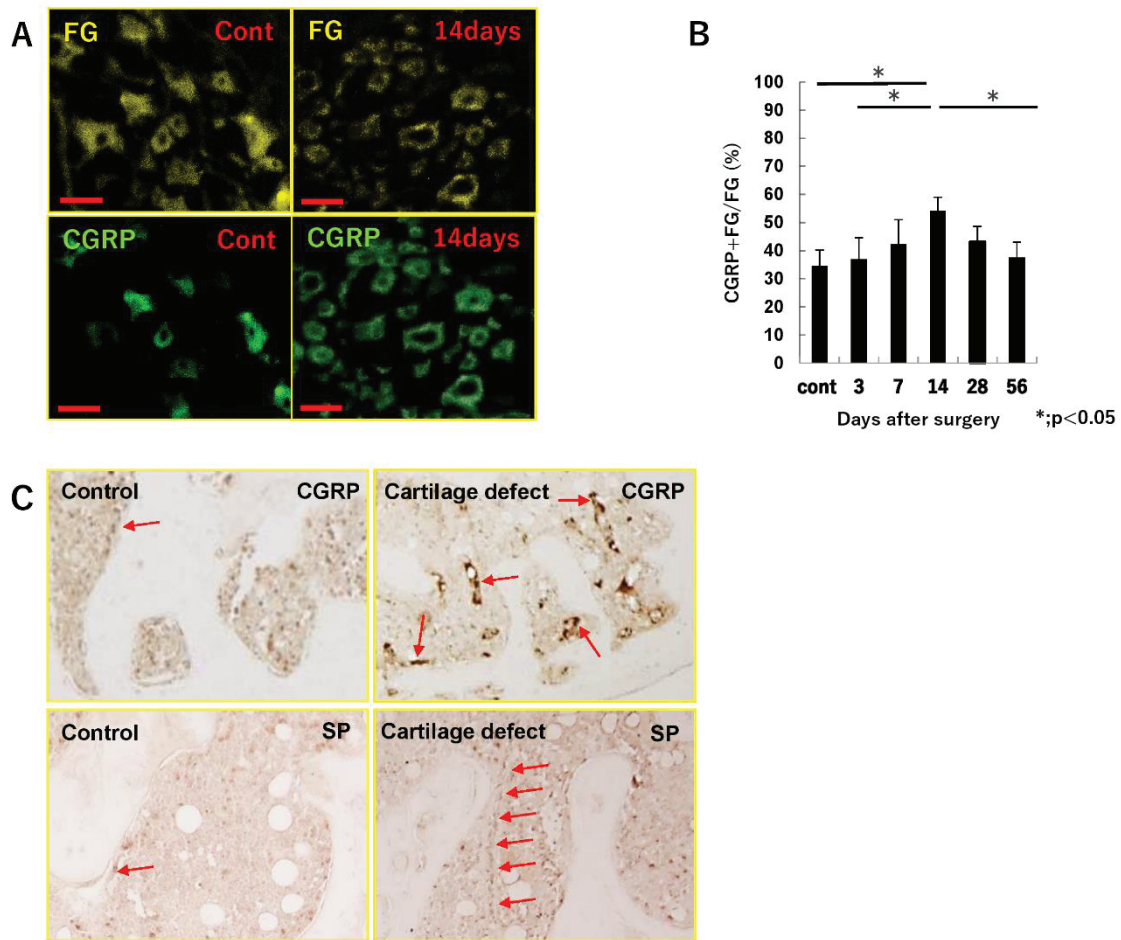
233 ***Pain Assessment***

234 Compared with the sham models, cartilage defect models showed significantly  
 235 reduced total distance traveled in the open field test on day 14 ( $P = 0.008$ ) and 56 ( $P =$   
 236  $0.00007$ ) (Figure 6A), and a reduced number of times of rearing on day 14 ( $P = 0.01$ )  
 237 (Figure 6B). In immunofluorescence staining for CGRP of the DRG, the percentage of  
 238 CGRP -and FG- positive fibers increased peaked on day 14, and gradually decreased from  
 239 day 28. The percentage measured on day 14 ( $54.1\% \pm 4.9\%$ ) was significantly higher than  
 240 that of the control group, and day3 and day56 ( $34.5\% \pm 5.6\%$ ,  $36.9\% \pm 7.6\%$ , and  $37.5\%$

241  $\pm 5.5\%$  for the control group, and days 3 and 56, respectively) (Figure 7A, 7B).  
 242 Immunostaining images for CGRP and substance P of the knee are shown in Figure 7C.  
 243 The number of fibers stained positively for CGRP and substance P positive increased in  
 244 the subchondral bone under the cartilage defect on day 14.



245  
 246 Figure 6. The results of the open field test; (A) total distance travelled, and (B) the number  
 247 of times rearing occurred.  
 248



249

250 Figure 7. (A) immunofluorescence staining for Fluoro-Gold(FG) and calcitonin gene-  
 251 related peptide (CGRP) of the dorsal root ganglion (DRG). The bar indicates a distance  
 252 of 50  $\mu$ m. (B) the percentage of CGRP-positive cells at each time. (C) immunostaining  
 253 for CGRP and substance P (SP) of the knee on the control group and day 14. The bar  
 254 indicates a distance of 50  $\mu$ m.

255

## 256 Discussion

257 The purpose of this study was to clarify the natural changes in the subchondral bone,

258 and the relationship between the condition of the subchondral bone and pain in the early  
259 phase of articular cartilage defects in a rat model. Our results suggest that the activation  
260 of osteoclasts occurred from day 7, bone resorption of subchondral bone peaked on day  
261 14, and subsequent bone sclerosis by osteoblast activation occurred from day 28. In  
262 addition, from the results of the open field test and immunofluorescence staining of the  
263 DRGs and subchondral bone, the pain level was estimated to peak at day 14, concomitant  
264 with bone absorption in the subchondral bone. Thus, the natural course of an articular  
265 cartilage defect in a rat model was revealed, and it was associated with pain levels. The  
266 findings of this study suggest that the condition of the subchondral bone can be inferred  
267 from radiographic assessment and pain level, and this will contribute to the treatment of  
268 cartilage defects in clinical practice.

269 The pathogenesis of pain due to articular cartilage defects is not fully understood,  
270 although several factors are thought to be involved in the process. Since articular cartilage  
271 does not have a nerve fiber, surrounding tissues such as the subchondral bone and  
272 synovium may cause pain. In particular, the subchondral bone under the cartilage defect  
273 is directly affected by the loading force, which may subsequently induce changes in the  
274 bone structure.<sup>19</sup> Also, the mechanism of pain experienced in OA and osteochondral  
275 lesions (OCLs) is better understood than that in cartilage defects. In OCLs, pain may

276 develop from the pressurized fluid into the subchondral bone, which induces decreasing  
277 pH caused by osteoclasts. A low pH excites the nerve fibers present in the bone, inducing  
278 pain.<sup>20</sup> In OA, the subchondral bone has received much attention as a cause of pain. In  
279 previous reports, subchondral bone marrow edema-like lesions were visualized using  
280 magnetic resonance imaging, and were highly correlated with OA pain.<sup>21,22</sup> It has also  
281 been reported that an increase in osteoclast-mediated bone resorption induces sensory  
282 innervation in the subchondral bone and hyperexcitability of DRG neurons, which  
283 induces OA pain.<sup>23</sup> In clinical practice, risedronate, an osteoclast inhibitor, has been tested  
284 for use in OA and it has been shown to decrease subchondral bone marrow lesions, thus  
285 improving pain.<sup>24,25</sup> In this study, osteoclast activity under the cartilage defect was highest  
286 on day 14, suggesting a correlation between the course of pain and activation of  
287 osteoclasts.

288 Bone remodeling is continuously maintained through a tight equilibrium between  
289 osteoblast activity which is responsible for bone formation through the synthesis of bone  
290 matrix and osteoclast activity which is responsible for degrading the bone  
291 microenvironment.<sup>26</sup> In this study, osteoclasts situated under the cartilage defects were  
292 activated from days 7 to 14, and osteoblasts were activated from day 7, suggesting that  
293 the metabolism of the subchondral bone was enhanced after the articular cartilage defect

294 was created. It is well known that osteoclasts below the cartilage are activated due to the  
295 increased load, inducing subchondral bone loss in early-stage OA, and subchondral bone  
296 becomes sclerotic at a later stage of OA.<sup>27,28</sup> Our results suggest that subchondral bone  
297 remodeling after cartilage defect is similar to that observed in the pathogenesis of OA.  
298 Previous reports have shown that subchondral bone plays an important role in maintaining  
299 cartilage homeostasis,<sup>3</sup> and damage to the subchondral bone causes the progression of  
300 cartilage damage vice versa.<sup>29</sup> Furthermore, cartilage destruction in anterior cruciate  
301 ligament transection models is secondary to subchondral bone damage. However, the  
302 mechanism of the naturally-occurring OA induced by collagenase injection is suggested  
303 that the absorption of subchondral bone is secondary to cartilage lesions.<sup>30</sup> In summary,  
304 the condition of the subchondral bone is related to the condition of the cartilage, and the  
305 condition of the subchondral bone affects the repair of cartilage.

306 Subchondral bone cysts are a major complication of the microfracture technique for  
307 cartilage defects.<sup>7</sup> Our results suggest that microfracture in an osteoclast-dominated  
308 situation, such as on day 14 after damage to the cartilage, may cause subchondral bone  
309 cysts to develop. After an acute traumatic articular cartilage injury, the cartilage lesion  
310 might best be treated within 2 weeks after injury to prevent subchondral bone  
311 deterioration due to osteoclast activation by careful weight-bearing control to reduce the

312 influx of joint fluid. Therefore, understanding the change in the condition of the  
313 subchondral bone will result in the successful treatment of damaged cartilage defects.  
314 Imaging examinations such as CT and MRI are used to understand the condition of the  
315 subchondral bone in clinical practice. In addition, the pain level can be a monitoring tool  
316 for subchondral bone conditions. It is reported that antiresorptive drugs such as  
317 bisphosphonates are well known to be useful for OA pain and OA progression.<sup>31,32</sup> These  
318 findings, in addition to our results, support the hypothesis that drugs targeting osteoclasts  
319 can potentially inhibit pain and changes in the subchondral bone in the early stages after  
320 damage to the cartilage. Besides, further studies will be required to develop surgical  
321 procedures such as microfracture technique by analyses of the actual changes of the  
322 subchondral bone seen after microfracture and to investigate the feasibility of the  
323 application of biomaterials to improve the therapeutic repair outcomes including pain  
324 reduction.

325 This study has several limitations. First, we used rats as the animal model. Since the  
326 rate of bone metabolism differs between humans and rats, the time course of changes in  
327 the subchondral bone after cartilage injury may be different from that in humans.  
328 Moreover, many factors affect subchondral bone changes, such as age, sex, and degree or  
329 location of, or intervention for the cartilage injury. Second, all the animals could move

330 freely after the cartilage defect was created in their limb, which may have affected the  
331 rate of metabolism in the subchondral bone.<sup>33</sup> These factors may have affected the results  
332 of this study. Therefore, the bone resorption phase may start later than 2 weeks after  
333 cartilage injury. However, the process in which subchondral bone resorption occurs and  
334 then it changes toward bone formation as sclerotic change after cartilage injury remains  
335 unchanged, and cartilage injury should be appropriately treated according to the condition  
336 of the subchondral bone to achieve good clinical results.

337 In conclusion, the condition of the subchondral bone under an articular cartilage  
338 defect dynamically changes from bone resorption to sclerosis, and this process is related  
339 to the level of pain experienced. Appropriate intervention for the cartilage defect by taking  
340 into account the subchondral bone changes and their relationship with pain, will enable  
341 patients with articular cartilage injury to be treated successfully.

342

### 343 **References**

- 344 1. Correa D, Lietman SA. Articular cartilage repair: Current needs, methods and  
345 research. *Seminars in cell & Developmental biology*. 2017;62:67-77.
- 346 2. Safran MR, Seiber K. The evidence for surgical repair of articular cartilage in the  
347 knee. *J Am Acad Orthop Surg*. 2010;18(5):259-266.

- 348 3. Buckwalter JA, Mankin HJ. Articular cartilage: tissue design and chondrocyte-matrix  
349 interactions. *Instr Course Lect.* 1998;47:477-486.
- 350 4. Ding C, Cicuttini F, Jones G. How important is MRI for detecting early osteoarthritis?  
351 *Nat Clin Pract Rheumatol.* 2008;4(1):4-5.
- 352 5. Hinckel BB, Thomas D, Vellios EE, Hancock KJ, Calcei JG, Sherman SL, et al.  
353 Algorithm for treatment of focal cartilage defects of the knee: Classic and new  
354 procedures. *Cartilage.* 2021 Mar 20:1947603521993219.
- 355 6. Steadman JR, Briggs KK, Rodrigo JJ, Kocher MS, Gill TJ, Rodkey WG. Outcomes  
356 of microfracture for traumatic chondral defects of the knee: average 11-year follow-  
357 up. *Arthroscopy.* 2003;19(5):477-484.
- 358 7. Minas T, Gomoll AH, Rosenberger R, Royce RO, Bryant T. Increased failure rate of  
359 autologous chondrocyte implantation after previous treatment with marrow  
360 stimulation techniques. *Am J Sports Med.* 2009;37(5):902–908.
- 361 8. Hayashi S, Nakasa T, Ishikawa M, Nakamae A, Miyaki S, Adachi N. Histological  
362 evaluation of early-phase changes in the osteochondral unit after microfracture in a  
363 full-thickness cartilage defect rat model. *Am J Sports Med.* 2018 46(12):3032-3039.
- 364 9. Burr DB. Anatomy and physiology of the mineralized tissues: role in the  
365 pathogenesis of osteoarthrosis. *Osteoarthritis Cartilage.* 2004;12 Suppl A:S20 – S30.

- 366 10. van Dijk CN, Relingh ML, Zengerink M, van Bergen CJA. The natural history of  
367 osteochondral lesions in the ankle. *Instr Course Lect.* 2010;59:375-386.
- 368 11. Yu D, Liu F, Liu M, Zhao X, Wang X, Li Y, et al. The inhibition of Subchondral Bone  
369 Lesions Significantly Reversed the Weight-Bearing Deficit and the Overexpression  
370 of CGRP in DRG Neurons, GFAP and Iba-1 in the Spinal Dorsal Horn in the  
371 Monosodium Iodoacetate Induced Model of Osteoarthritis Pain. *PLoS One.*  
372 2013;8(10):e77824.
- 373 12. Sun Q, Zhen G, Li TP, Guo Q, Li Y, Su W et al. Parathyroid hormone attenuates  
374 osteoarthritis pain by remodeling subchondral bone in mice. *Elife* 2021 Mar  
375 1;10:e65532.
- 376 13. Miyamoto A, Deie M, Yamasaki T, Nakamae A, Shinomiya R, Adachi N. The role of  
377 the synovium in repairing cartilage defects. *Knee Surg Sports Traumatol Arthrosc.*  
378 2007;15(9):1083-1093.
- 379 14. Ferreira-Gomes J, Adaes S, Sarkander J, Castro-Lopes JM. Phenotypic alterations of  
380 neurons that innervate osteoarthritic joints in rats. *Arthritis*  
381 *Rheum.* 2010;62(12):3677–3685.
- 382 15. Hoshino T, Tsuji K, Onuma H, Udo M, Ueki H, Akiyama M, et al. Persistent synovial  
383 inflammation plays important roles in persistent pain development in the rat knee

- 384 before cartilage degradation reaches the subchondral bone. *BMC Musculoskeletal*  
385 *Disorders*. 2018;19(1):291.
- 386 16. Aho OM, Finnilä M, Thevenot J, Saarakkala S, Lehenkari P. Subchondral bone  
387 histology and grading in osteoarthritis. *PLoS One*. 2017;12(3):e0173726.
- 388 17. Lacourt M, Gao C, Li A, Girard C, Beauchamp G, Henderson JE, et al. Relationship  
389 between cartilage and subchondral bone lesions in repetitive impact trauma-induced  
390 equine osteoarthritis. *Osteoarthr Cartil*. 2012;20(6):572-83.
- 391 18. Crumeyrolle-Arias M, Jaglin M, Bruneau A, Vancassel S, Cardona A, Dauge V, et al.  
392 Absence of the gut microbiota enhances anxiety-like behavior and neuroendocrine  
393 response to acute stress in rats. *Psychoneuroendocrinology*. 2014;42:207–217.
- 394 19. Hayes DW Jr, Brower RL, John KJ. Articular cartilage. Anatomy, injury, and repair.  
395 *Clin Podiatr Med Surg*. 2001;18(1):35-53.
- 396 20. van Dijk CN, Relingh ML, Zengerink M, van Bergen CJ. Osteochondral defects in  
397 the ankle: why painful? *Knee Surg Sports Traumatol Arthrosc*. 2010;18(5):560-580.
- 398 21. Kwok CK. Clinical relevance of bone marrow lesions in OA. *Nat Rev Rheumatol*.  
399 2013;9(1):7–8.35.
- 400 22. Yusuf E, Kortekaas MC, Watt I, Huizinga TW, Kloppenburg M. Do knee  
401 abnormalities visualized on MRI explain knee pain in knee osteoarthritis? A

402 systematic review. *Ann Rheum Dis.*2011;70(1):60–67.

403 23. Zhu S, Zhu J, Zhen G, Hu Y, An S, Li Y, et al. Subchondral bone osteoclasts induce  
404 sensory innervation and osteoarthritis pain. *J Clin Invest.* 2019;129(3):1076-1093.

405 24. Buckland-Wright JC, Messent EA, Bingham CO, Ward RJ, Tonkin C. A 2 yr  
406 longitudinal radiographic study examining the effect of a bisphosphonate  
407 (risedronate) upon subchondral bone loss in osteoarthritic knee patients.  
408 *Rheumatology (Oxford).* 2007;46(2):257–264.

409 25. Spector TD, Conaghan PG, Buckland-Wright JC, Garnero P, Cline GA, Beary JF, et  
410 al. Effect of risedronate on joint structure and symptoms of knee osteoarthritis: results  
411 of the BRISK randomized, controlled trial [ISRCTN01928173]. *Arthritis Res*  
412 *Ther.*2005;7(3):R625–R633.

413 26. Kwan Tat S, Lajeunesse D, Pelletier JP, Martel-Pelletier J. Targeting subchondral  
414 bone for treating osteoarthritis: what is the evidence? *Best Pract Res Clin*  
415 *Rheumatol.* 2010;24(1):51-70.

416 27. Botter SM, van Osch GJVM, Clockaerts S, Waarsing JH, Weinans H, van Leeuwen  
417 JPTM. Osteoarthritis induction leads to early and temporal subchondral plate  
418 porosity in the tibial plateau of mice: an in vivo microfocal computed tomography  
419 study. *Arthritis Rheum.* 2011; 63(9):2690-2699.

- 420 28. Pastoureau PC, Bonnet ACC. Evidence of early subchondral bone changes in the  
421 meniscectomized guinea pig. A densitometric study using dual energy X-ray  
422 absorptiometry subregional analysis. *Osteoarthritis Cartilage*. 1999;7(5):466-473.
- 423 29. Radin EL, Rose RM. Role of subchondral bone in the initiation and progression of  
424 cartilage damage. *Clin Orthop Relat Res*. 1986;(213):34-40.
- 425 30. Yang Y, Li P, Zhu S, Bi R. Comparison of early-stage changes of osteoarthritis in  
426 cartilage and subchondral bone between two different models. *Peer J*. 2020;8:e8934.
- 427 31. Jones MD, Tran CW, Li G, Maksymowych WP, Zernicke RF, Doschak MR. In vivo  
428 microfocal computed tomography and micro-magnetic resonance imaging evaluation  
429 of antiresorptive and antiinflammatory drugs as preventive treatments of  
430 osteoarthritis in the rat. *Arthritis Rheum*. 2010;62(9):2726–2735.
- 431 32. Laslett LL, Doré DA, Quinn SJ, Boon P, Ryan E, Winzenberg TM, et al. Zoledronic  
432 acid reduces knee pain and bone marrow lesions over 1 year: a randomised controlled  
433 trial. *Ann Rheum Dis*. 2012;71(8):1322–1328.
- 434 33. Oettmeier R, Arokoski J, Roth AJ, Helminen HJ, Tammi M, Abendroth K.  
435 Quantitative study of articular cartilage and subchondral bone remodeling in the knee  
436 joint of dogs after strenuous running training. *J Bone Miner Res*. 1992;7:S419-S424.  
437